

# OPIRL: Sample Efficient Off-Policy Inverse Reinforcement Learning via Distribution Matching

Hana Hoshino<sup>1</sup>, Kei Ota<sup>1,2</sup>, Asako Kanezaki<sup>1</sup> and Rio Yokota<sup>3</sup>

**Abstract**—Inverse Reinforcement Learning (IRL) is attractive in scenarios where reward engineering can be tedious. However, prior IRL algorithms use on-policy transitions, which require intensive sampling from the current policy for stable and optimal performance. This limits IRL applications in the real world, where environment interactions can become highly expensive. To tackle this problem, we present Off-Policy Inverse Reinforcement Learning (OPIRL), which (1) adopts off-policy data distribution instead of on-policy and enables significant reduction of the number of interactions with the environment, (2) learns a stationary reward function that is transferable with high generalization capabilities on changing dynamics, and (3) leverages mode-covering behavior for faster convergence. We demonstrate that our method is considerably more sample efficient and generalizes to novel environments through the experiments. Our method achieves better or comparable results on policy performance baselines with significantly fewer interactions. Furthermore, we empirically show that the recovered reward function generalizes to different tasks where prior arts are prone to fail.

**Index Terms**—Imitation Learning, Transfer Learning, Learning from Demonstration, Inverse Reinforcement Learning.

## I. INTRODUCTION

Imitation learning (IL) seeks to adopt optimal policies directly from expert demonstrations. It mitigates the challenge of explicit reward engineering where poor designs can lead to sub-optimal policies with disastrous behaviors [1]. Compared to conventional Reinforcement Learning (RL) algorithms, IL only requires expert examples, which can be much simpler to obtain desired behaviors than providing hand-crafted rewards. This can be highly appealing in many real-world scenarios where designing a reward function to achieve ideal behaviors requires tremendous effort or is even infeasible in complex systems, *e.g.*, autonomous robots [2], trajectory prediction [3], and autonomous driving [4], etc.

Towards robust imitations, recent works on IL have integrated adversarial learning [5] which have shown to be highly efficient and effective. These methods *implicitly* infer a non-stationary reward by training a discriminator in the form of generative adversarial networks (GAN) [6], and updates the policy using the reward derived from the discriminator. However, IL methods are widely known to not generalize outside the environment where it was trained on [7, 8]. On the other hand, emerging from the same motivation as

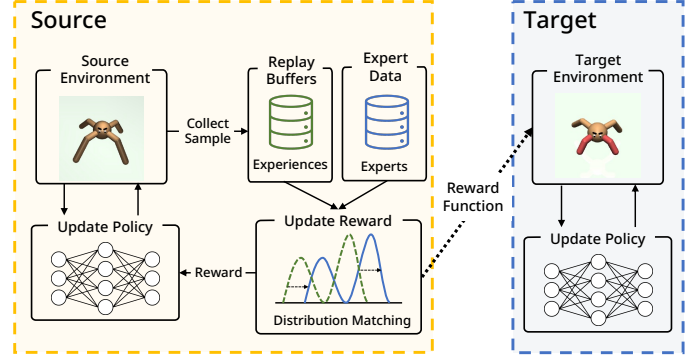


Fig. 1: **Overview of OPIRL framework:** OPIRL (1) achieves high sample efficiency and (2) recovers a robust reward function that can be transferred and generalize across different environment by applying off-policy training in distribution matching.

IL, Inverse Reinforcement Learning (IRL) [9, 10] aims to infer a stationary reward function from expert demonstrations to train the agent policy. The inferred reward functions by IRL can be transferred to different environments. As reward functions that define the underlying intention of the experts are portable, an agent can be re-optimized in changing dynamics. Hence, IRL shows high generalization capability to different environments [7, 11].

Although seemingly pleasant and appealing, IRL still has multiple problems, such as ambiguity in reward functions [10] and sample inefficiency [12, 13]. In our paper, a “sample efficient manner” indicates that an agent requires fewer interactions with the environment, in contrast to some other papers implying the number of expert demonstrations needed to learn optimal reward/policy [8]. In this work, we mainly look into the sample inefficiency of IRL. Prior arts such as AIRL [7] require a large amount of expert data and frequent interactions with the environment to recover optimal reward function and policy due to its *on-policy* training. As on-policy methods rely on Monte Carlo estimations, it suffers from high variance in gradient estimates, which is subsided via intensive sampling [14, 15]. However, exhaustive interactions with the environment can become expensive. *Off-policy* transitions can mitigate the issue by storing previous samples in a replay-buffer instead of intensively collecting a large amount of on-policy experience after each policy update. In the context of IL, several *off-policy* algorithms have been proposed [15–18]. Especially, OPOLO [18] removes *on-policy* dependencies in distribution matching via equation transformation. Nonetheless, no IRL methods have theoretically derived an off-policy IRL algorithm with portable

<sup>1</sup> School of Computing, Department of Computer Science, Tokyo Institute of Technology, Japan.

<sup>2</sup> Information Technology R&D Center, Mitsubishi Electric Corporation, Japan.

<sup>3</sup> Global Scientific Information and Computing Center, Tokyo Institute of Technology, Japan.

reward functions.

Recent works on IRL shed light on distribution matching [19], which aims to minimize the difference of stationary distributions between the expert and the learned agent. Prior approaches use *on-policy* samples in order to obtain an accurate distribution of the learning policy. Inspired by OPOLO, we formulate Off-Policy Inverse Reinforcement Learning (OPIRL) based on the idea of distribution matching and Adversarial Inverse Reinforcement Learning (AIRL). Furthermore, to encourage active explorations at the beginning stages of training, we adopt mode-covering behavior [20] by integrating behavior cloning loss and Q-Filter [21]. OPIRL holds each desired property of prior IL and IRL methods: OPIRL (1) achieves high sample efficiency like recent off-policy IL methods, and (2) generalizes to unseen environments like prior IRL methods. We demonstrate that OPIRL shows state-of-the-art results on policy performance benchmarks while reducing the interactions with the environment. Due to the nature of off-policy sampling, where it updates policy using data sampled from a wide variety of distributions, our algorithm achieves expert-level performance with a *single* expert trajectory, in contrast to prior IRL methods, which require multiple trajectories. Furthermore, we demonstrate that OPIRL can generalize to different environments by inferring a transferable reward function, while other IRL methods could not reach the performance of OPIRL, and IL methods fail to generalize. Implementations of OPIRL is available at <https://github.com/sff1019/opirl>.

## II. RELATED WORK

**Inverse reinforcement learning** is a problem setting to learn a reward function from a set of expert trajectories [10]. MaxEntIRL recovers stationary reward functions by minimizing the forward KL divergence in trajectory space under the maximum entropy RL framework [22]. To retrieve policy while learning reward functions directly, recent works combine generative adversarial network (GAN) [6] to training. GAN-GCL [23] uses GAN to optimize an MLE objective over trajectories. AIRL [7] improves upon this to recover a reward function while simultaneously learning the policy. Instead of using adversarial learning, *f*-IRL [24] solves the state marginal matching problem to infer the reward function. Although such works show prominent improvement in robustness and performance, many remain data-hungry due to the on-policy data transitions.

**Imitation learning** does not recover reward functions, instead it tries to acquire optimal policy from demonstrations provided by an expert policy. GAIL [5] uses the GAN formulation in training, allowing it to be more sample efficient than behavior cloning (BC) in terms of the number of expert demonstrations. However, similar to IRL methods, it suffers sample-inefficiency. To mitigate this problem, several *off-policy* IL methods have recently been proposed. Sample-efficient Adversarial Mimic (SAM) [15] uses off-policy actor-critic to remove the on-policy dependencies. Sasaki et al. [16] propose an algorithm that incorporates an off-policy actor-critic algorithm to optimize the policy. Simi-

larly, Discriminator-Actor-Critic (DAC) [12], an extension of GAIL, uses observations stored in the replay buffer, instead of on-policy transitions for its policy updates. Nonetheless, although DAC shows empirically better results in terms of sample efficiency, it deviates from its theoretically correct objective because it ignores computing the importance sampling term. To remove such discrepancy, several off-policy IL methods utilize distribution matching algorithms: ValueDICE [17] and OPOLO [18]. ValueDICE incorporates distribution correction estimation [25] to remove on-policy dependency. However, the policy objective contains logarithms and exponential expectations, which introduce biases in its gradients [26]. On the other hand, OPOLO adopts an off-policy transition to IL in principle manner by deriving an upper-bound of the IL objective, which removes such biases.

Our work is built on the findings of OPOLO to improve sample efficiency in inverse reinforcement learning framework while recovering reward functions to achieve high generalization across different environments, which imitation learning methods (*e.g.*, DAC, OPOLO, etc.) are prone to fail.

## III. PRELIMINARIES

We consider a Markov Decision Process (MDP), defined by the tuple  $(\mathcal{S}, \mathcal{A}, \mathcal{P}, r, \rho_0, T)$ , where  $\mathcal{S}$  and  $\mathcal{A}$  denote the state and action space, dynamics  $\mathcal{P} : \mathcal{S} \times \mathcal{A}$ ,  $r(s, a)$  as the reward function, initial state-action distribution  $\rho_0(s, a)$ , and horizon  $T$ . The goal of *forward* reinforcement learning is to find the optimal policy  $\pi^*$  that maximizes the expected entropy-regularized discounted reward [22]:

$$\pi^* = \operatorname{argmax}_{\pi} \mathbb{E}_{\rho_{\pi}(s, a)} \left[ \sum_{t=0}^T \gamma^t (r(s_t, a_t) + \alpha \mathcal{H}(\pi(\cdot|s_t))) \right] \quad (1)$$

where  $\rho_{\pi}$  is the state-action distribution, and  $\alpha > 0$  is the entropy temperature.

*Inverse* reinforcement learning instead seeks to infer the reward function  $r(s, a)$  from a given set of demonstrations  $\mathcal{D} = \{\tau_1, \dots, \tau_N\}$  from an expert policy  $\pi_{\text{exp}}$ , where  $\tau$  is the trajectory. MaxEntIRL [22], a method built on the maximum entropy RL framework, can be interpreted as solving the maximum likelihood problem:

$$\max_{\theta} J(\theta) = \max_{\theta} \mathbb{E}_{\tau \sim \mathcal{D}} [\log \rho^{\pi_{\theta}}(\tau)] \quad (2)$$

where  $p_{\theta}(\tau) \propto p(s_0) \sum_{t=0}^T p(s_{t+1}|s_t, a_t) \exp(r(s, a)/\alpha)$ . Adversarial Inverse Reinforcement Learning (AIRL) [7] involves GAN formulation to acquire solution for MaxEntIRL. The discriminator in AIRL is structured as

$$D_{\omega, \Phi}(s, a) = \frac{\exp(h_{\omega, \Phi}(s, a))}{\exp(h_{\omega, \Phi}(s, a) + \pi_{\theta}(a|s))} \quad (3)$$

where  $h_{\omega, \Phi}(s, a) = r_{\omega}(s, a) + \gamma V_{\Phi}(s') - V_{\Phi}(s)$ , reward function  $r_{\omega}(s, a)$ , and value function  $V_{\Phi}(s)$  and  $V_{\Phi}(s')$ . In AIRL, the policy optimizes

$$\mathbb{E}_{(s_t, a_t) \sim \pi} \left[ \sum_t \log D_{\omega, \Phi}(s_t, a_t) - \log(1 - D_{\omega, \Phi}(s_t, a_t)) \right]. \quad (4)$$

This can be interpreted as solving MaxEntIRL problem by minimizing the reverse KL-Divergence,  $\min \text{KL}(\rho^{\pi_\theta}(s, a) \parallel \rho^{\text{exp}}(s, a))$ , where  $\rho^{\pi_\theta}$  and  $\rho^{\text{exp}}$  are the state-action distribution of the current agent and the expert respectively [19].

#### IV. OPIRL: OFF-POLICY INVERSE REINFORCEMENT LEARNING VIA DISTRIBUTION MATCHING

In this section, we will introduce our algorithm: OPIRL. We first show how we incorporate off-policy learning in adversarial inverse reinforcement setting, and then show how we improve the efficiency to train OPIRL.

##### A. Off-policy Learning in Inverse Reinforcement Learning

As stated in Sec. III, AIRL minimizes the divergence between agent and expert state-action distribution. However, this training process can become sample-inefficient as computing the state-action distribution of the agent requires *on-policy* interactions with the environment. To resolve this issue, we will adopt *off-policy* distribution  $\rho^R(s, a)$  into our objective function. The reverse KL-Divergence between agent and expert state-action distribution can be rewritten using state-action distribution of the replay-buffer  $\rho^R$ :

$$\begin{aligned} \text{KL}(\rho^{\pi_\theta}(s, a) \parallel \rho^{\text{exp}}(s, a)) \\ = \mathbb{E}_{\rho^{\pi_\theta}} \left[ \log \frac{\rho^R(s, a)}{\rho^{\text{exp}}(s, a)} \right] + \text{KL}(\rho^{\pi_\theta}(s, a) \parallel \rho^R(s, a)) \end{aligned} \quad (5)$$

where the replay-buffer [27] is a structure used in many off-policy learning methods in which past experiences are re-used to improve sample efficiency and performance.

Although KL-Divergence is used in many applications, it is known to have biases in gradients [26]. Especially, the expectation of a logarithm and exponential yields biases in mini-batch training. Hence, to avoid this issue we instead calculate an upper-bound of KL-divergence using Jensen's inequality.

$$\text{KL}(P \parallel Q) \leq \mathbb{D}_f(P \parallel Q). \quad (6)$$

This holds true when a convex function  $f(x)$  is  $f(x) = \frac{1}{p}|x|^p$ . Built upon this transformation, our new objective function can be derived using  $f$ -Divergence:

$$\min_{\pi} J(\theta) := \mathbb{E}_{\rho^{\pi_\theta}} \left[ \log \frac{\rho^R(s, a)}{\rho^{\text{exp}}(s, a)} \right] + \mathbb{D}_f[\rho^{\pi_\theta}(s, a) \parallel \rho^R(s, a)]. \quad (7)$$

However, the agent state-action distribution  $\rho^{\pi_\theta}$  still remains, thus requires *on-policy* distribution. Following the works of Nachum et al. [28] and Zhu et al. [18], we first leverage the dual-form of  $f$ -divergence:

$$\begin{aligned} -\mathbb{D}_f[\rho^{\pi_\theta}(s, a) \parallel \rho^R(s, a)] \\ = \inf_{x: S \times \mathcal{A} \rightarrow R} \mathbb{E}_{\rho^{\pi_\theta}} [-x(s, a)] + \mathbb{E}_{\rho^R} [f_*(x(s, a))] \end{aligned} \quad (8)$$

where  $f_*(\cdot)$  is the convex conjugate of  $f(\cdot)$ . Using this dual form, we can rewrite our objective function as:

$$\begin{aligned} \min J(\theta) &:= \max_{\pi} \mathbb{E}_{\rho^{\pi_\theta}} \left[ -\log \frac{\rho^R(s, a)}{\rho^{\text{exp}}(s, a)} \right] \\ &\quad - \mathbb{D}_f[\rho^{\pi_\theta}(s, a) \parallel \rho^R(s, a)] \\ &= \max_{\pi} \mathbb{E}_{\rho^{\pi_\theta}} \left[ \log \frac{\rho^{\text{exp}}(s, a)}{\rho^R(s, a)} - x(s, a) \right] \\ &\quad - \mathbb{E}_{\rho^R} [f_*(x(s, a))]. \end{aligned} \quad (9)$$

If we consider a synthetic reward as  $\mathcal{R}(s, a) = \log \frac{\rho^{\text{exp}}(s, a)}{\rho^R(s, a)} - x(s, a)$ , the first term in Eq. (9) can be interpreted as an RL return function:  $\max_{\pi} \hat{J}(\pi) = \max \mathbb{E}_{(s, a) \sim \rho^{\pi_\theta}(s, a)} [\mathcal{R}(s, a)]$ . In RL, the Q-value function is written in the following form:

$$Q_\phi(s, a) = \mathbb{E}_{\rho^{\pi_\theta}} [\mathcal{R}(s, a) + \gamma Q_\phi(s', a')]. \quad (10)$$

Inspired by OPOLO [18], we make a change in variables by learning the Q-function:

$$\begin{aligned} Q_\phi(s, a) &= -x(s, a) + \mathbb{E}_{\rho^{\pi_\theta}} \left[ \log \frac{\rho^{\text{exp}}(s, a)}{\rho^R(s, a)} + \gamma Q_\phi(s', a') \right] \\ &= -x(s, a) + \mathcal{B}^\pi Q_\phi(s, a) \end{aligned}$$

where  $\mathcal{B}^\pi$  is the expected Bellman operator with respect to  $\pi$ . Applying  $x(s, a) = (\mathcal{B}^\pi Q_\phi - Q_\phi)(s, a)$ , our objective function can be written without the *on-policy* expectation:

$$\begin{aligned} \max_{\pi} \min_{x: S \times \mathcal{A} \rightarrow R} J(\pi, x) \\ = \max_{\pi} \min_{Q: S \times \mathcal{A} \rightarrow R} J(\pi, Q_\phi) \\ = \mathbb{E}_{\rho^{\pi_\theta}} \left[ \log \frac{\rho^{\text{exp}}(s, a)}{\rho^R(s, a)} - (\mathcal{B}^\pi Q_\phi - Q_\phi)(s, a) \right] \\ + \mathbb{E}_{\rho^R} [f_*((\mathcal{B}^\pi Q_\phi - Q_\phi)(s, a))] \\ = (1 - \gamma) \mathbb{E}_{s_0, a_0} [Q(s_0, a_0)] \\ + \mathbb{E}_{\rho^R} [f_*((\mathcal{B}^\pi Q_\phi - Q_\phi)(s, a))]. \end{aligned} \quad (11)$$

This final objective function is fully *off-policy*, thus can be trained by using off-policy transitions sampled from replay-buffer  $\rho^R$ . We can estimate  $\log \frac{\rho^{\text{exp}}(s, a)}{\rho^R(s, a)}$  in  $\mathcal{B}^\pi Q$ , which is the reward, by inferring it from the reward function trained through adversarial learning.

##### B. Learning Rewards via Inverse Reinforcement Learning

We use the same discriminator structure as AIRL (Eq. (3)). Through the training of this discriminator, we can obtain an explicit reward function, unlike prior works [17, 18].

Recent improvements on AIRL have provided multiple forms of the reward function. Especially, the original AIRL paper uses the following form:

$$\begin{aligned} \tilde{r}_{\omega, \Phi}(s, a) &= \log D_{\omega, \Phi}(s, a) - \log(1 - D_{\omega, \Phi}(s, a)) \\ &= h_{\omega, \Phi}(s, a) - \log \pi_\theta(a|s), \end{aligned} \quad (12)$$

which can be interpreted as an entropy regularized reward function. Following empirical findings in [29, 30], we remove the entropy regularized term in Eq. (12) and use the form

$$\tilde{r}_{\omega, \Phi}(s, a) = r_\omega(s, a). \quad (13)$$

### C. Modification for Efficient Training

In order to improve the efficiency of the training, we add two modifications to the objective function Eq. (11).

First, we modify the policy updates. It is widely known that adding an entropy regularization in policy updates improves performance in continuous control tasks [28, 31]. Therefore, we modify the rewards in the objective function Eq. (11) with a causal entropy term  $\log \pi(a|s)$

$$J(\pi_\theta, Q_\phi) = (1 - \gamma) \mathbb{E}_{s \sim s_0} [Q_\phi(s, \pi_\theta(s))] + \mathbb{E}_{(s,a) \sim \rho^R(s,a)} [f_*(\delta(s, a, r, s', a'))], \quad (14)$$

where  $s'$  and  $a'$  are the next state and action sampled from the policy, and

$$\delta(s, a, r, s', a') = \tilde{r}_{\omega, \Phi}(s, a) - \eta \log \pi_\theta(a'|s') + \gamma Q_\phi(s', a') - Q_\phi(s, a), \quad (15)$$

where  $\eta$ , also known as the temperature variable in [32], is learned during training.

Secondly, we adopt mode-covering behaviors in our policy updates [18, 20, 33]. Ghasemipour *et al.* [19] hypothesized that a mode-seeking behavior, which can be seen in reverse KL-Divergence such as ours, is desirable in RL scenarios as it cares more about the trajectories where the expert has visited. However, such behavior is less likely to explore regions expert has not covered. It tends to fall into local optimum, resulting in sub-optimal performance [20]. On the other hand, mode-covering enables policies to explore more widely. Mode-covering can be achieved via forward KL-Divergence, such as behavior cloning. Hence, we incorporate Behavior Cloning Loss [21, 34] into our policy updates to encourage active exploration at the beginning stages of training. We also add Q-Filter to avoid sub-optimal actions being chosen.

$$L_{BC} = \begin{cases} (\pi(s_i) - a_i)^2, & \text{if } Q_\phi(s_i, a_i) \leq Q_\phi(s_i, \pi(s_i)) \\ 0, & \text{otherwise.} \end{cases} \quad (16)$$

We empirically show that the combination of BC loss with Q-Filter enables OPIRL to achieve expert-level performance faster than without them. We show the overview of our algorithm in Algorithm 1.

### V. EXPERIMENTS

To evaluate the performance of our proposed algorithm, we conduct experiments to address the following questions:

- 1) **Policy Performance:** Can OPIRL recover the expert policy on imitation learning tasks with a smaller number of interactions with the environment?
- 2) **Reward Robustness:** Can OPIRL learn a robust reward function that can be transferred to environments that have different structures or dynamics?

To answer these questions, we compare our algorithm against IL methods that directly learn the policy: Behavior Cloning (BC), OPOLO<sup>1</sup> and DAC, and IRL methods that

---

### Algorithm 1: OPIRL: Off-Policy IRL

---

**Input:** A set of expert trajectories  $\tau_i^E$   
Initialize policy  $\pi_\theta$ , Discriminator  $D_{\omega, \Phi}$ , and critic  $Q_\phi$ .  
**for** step  $t$  in  $\{1, \dots, N\}$  **do**  
  Collect trajectories  $\tau_i = (s_0, a_0, \dots, s_T, a_T)$  by executing  $\pi$ .  
  Train discriminator  $D_{\omega, \Phi}$  via binary logistic regression to classify expert data  $\tau_i^E$  from samples  $\tau_i$ .  
  Infer reward  $\tilde{r}_{\omega, \Phi}$  from trained reward function  $r_\omega(s, a)$ .  
  Update  $\pi$  and  $Q_\phi$  with respect to  $\tilde{r}_{\omega, \Phi}(s, a)$ :  
    $J(\pi_\theta, Q_\phi) = (1 - \gamma) \mathbb{E}_{s \sim s_0} [Q_\phi(s, \pi_\theta(s)) + \mathbb{E}_{(s,a) \sim \rho^R(s,a)} [f_*(\tilde{r}_{\omega, \Phi}(s, a) - \eta \log \pi_\theta(a'|s') + \gamma Q_\phi(s', a') - Q_\phi(s, a))]]$   
   **if**  $Q(s, a) \leq Q(s, \pi_\theta(s))$  **then**  
     $L_{BC}(\pi_\theta) = (\pi_\theta(s) - a)^2$   
   **else**  
     $L_{BC}(\pi_\theta) = 0$   
   **end**  
    $\theta \leftarrow \theta - \alpha(\lambda_1 \nabla_\theta J + \lambda_2 \nabla_\theta L_{BC})$   
    $\phi \leftarrow \phi - \alpha \nabla_\phi J$   
**end**

---

learn the reward function and the policy:  $f$ -IRL<sup>2</sup>, and AIRL on commonly used MuJoCo locomotion tasks [35]. In particular, we use the variation of  $f$ -IRL, which uses forward KL-divergence, as it shows the most stable training [24]. Note that, OPOLO and DAC are off-policy IL methods. For each task, we train an agent using Soft-Actor-Critic (SAC) [31] as the expert policy, which is then used to collect a set of expert trajectories.

All networks are structured using 2-layered MLP with ReLU activation function and optimized using Adam. We use absorbing states of the environments following the works of Kostrikov *et al.* [12] and normalize states for stable training. For function  $f_*(x)$  in Eq. (11), we chose  $p = 1.5$  [25, 28]. For adversarial learning techniques, we use gradient penalty (GP) to avoid over-fitting the discriminator. Other options for discriminator regularization techniques include spectral normalization [36], Mixup [37, 38], and PUGAIL [39], however we chose GP as it has been empirically shown to achieve decent performance across multiple tasks [40, 41].

#### A. Policy Performance: MuJoCo Benchmarks

To evaluate whether OPIRL can acquire a policy that exhibits high performance like expert policy in a sample efficient manner, we compare OPIRL with other IL / IRL methods on five continuous control benchmark tasks within a 1 million step threshold. In addition, as collecting expert

<sup>1</sup><https://github.com/illidanlab/opolo-code>

<sup>2</sup><https://github.com/twni2016/f-IRL>

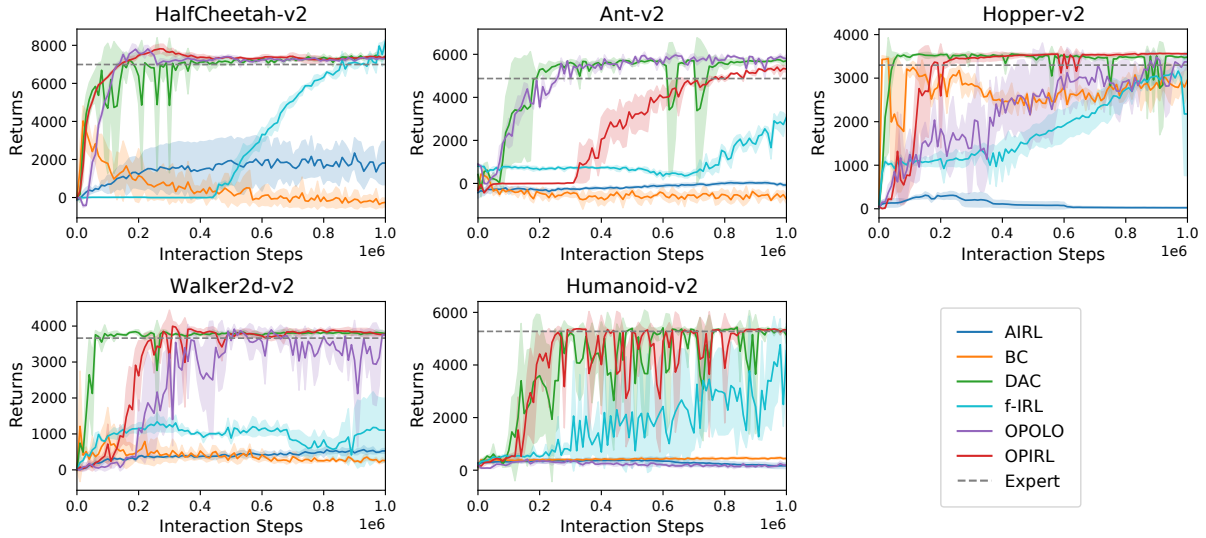


Fig. 2: Training curves of different algorithms using one expert trajectory. The expert policy performance is shown in a gray horizontal line, and we run each experiment independently with three seeds, and plot the average and  $\pm 1$  standard deviation with solid lines and shaded regions, respectively. OPIRL outperforms other IRL methods while achieving comparable performance with off-policy IL methods.

trajectories can sometimes require painful effort, it is desirable for agents to learn with a limited number of expert data. Therefore, we conduct this experiment using only one expert trajectory as similarly done in prior works [12, 24].

We show the learning curves of the average return using one expert trajectories in Fig. 2. It shows that OPIRL successfully recovers expert performance throughout the five tasks in very few steps, whereas  $f$ -IRL, which is the current state-of-the-art IRL method, requires much more steps to converge. We can also see that AIRL seems to fail on all tasks, similar to the findings of [24]. Thus, we confirm that OPIRL can achieve expert-level performance with fewer interactions with environments compared against prior IRL methods.

Next, we compare OPIRL to IL methods. BC also fails to recover a policy, which is mainly due to lack of training data as it is known to have a covariate-shift problem, hence requires multiple trajectories for robust learning [41]. Off-policy based IL methods, DAC and OPOLO, succeeded in recovering expert policy in all tasks, except for Humanoid with OPOLO. Overall, we can conclude that OPIRL can learn much more sample efficient than prior IRL methods such as AIRL and  $f$ -IRL, and perform comparably with off-policy IL algorithms. Furthermore, OPIRL succeeded in obtaining such performance with a single expert trajectory.

### B. Reward Robustness: Transfer Learning

To evaluate if OPIRL can learn a reward function that can generalize to different dynamics, we conducted experiments to see whether the recovered reward function in a source environment can be used in a target environment. We follow the setups of the AIRL paper [7]; we use the learned reward function from the source environment to re-train a policy on the target environment. As IL methods do not explicitly recover reward functions, we instead transfer the trained

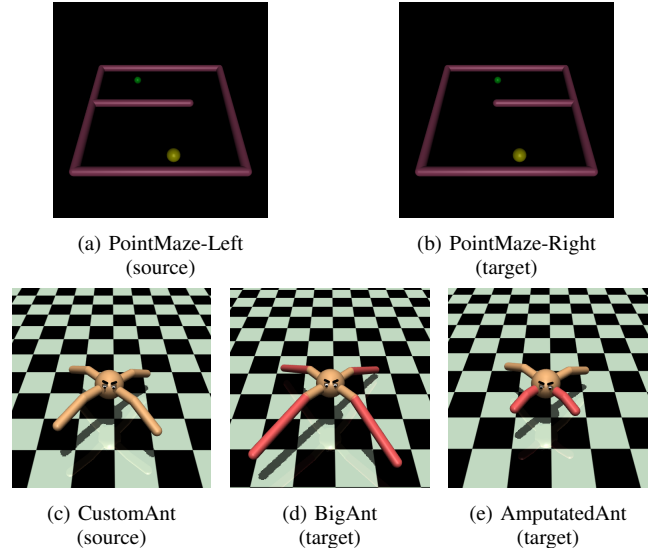


Fig. 3: The environments on which we evaluate the transfer capability of methods. Agents are trained on source environment (leftmost) and evaluated on the target environment (middle or right).

policy to the source environment to evaluate it on the target environment. We conducted experiments on two settings: 1) changing the environment structure, and 2) changing the dynamics of the environment (see Fig. 3).

The first task is evaluated on a 2D maze environment, where we control a point mass to navigate from start (yellow ball) to goal (green ball) while avoiding a barrier. The position of the barrier changes from left to right on test time (see Fig. 3a and Fig. 3b). The results in Table I clearly show that only OPIRL successfully solves the task in the target environments. On the other hand, although IL methods perform comparably with OPIRL on policy performance tasks, they perform poorly in reward robustness tasks. Other

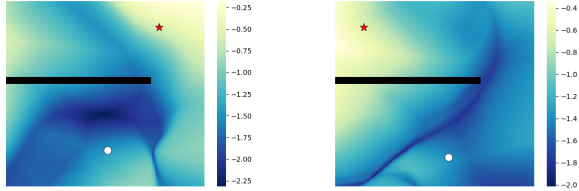


Fig. 4: Visualization of estimated reward function by using OPIRL. The white circle represents the agent, the red star represents the goal position, and the black rectangle shows the barrier.

TABLE I: Comparison between the final average return after transferring the reward function from source environments to target environments. Each method is evaluated using 20 episodes under 3 random seeds. <sup>†</sup> methods indicate results on direct policy generalization, and the bold number indicates the best score among each algorithm.

Method	PointMaze-Right	BigAnt	AmputatedAnt
DAC <sup>†</sup>	-36.2(±0.5)	8.6(±25.3)	-34.4(±24.7)
OPOLO <sup>†</sup>	-36.2(±0.5)	-18.8(±15.5)	-42.9(±7.3)
AIRL	-48.1(±14.2)	-36.8(±38.1)	25.4(±21.3)
<i>f</i> -IRL	-105.9(±34.4)	588.3(±369.4)	385.6(±57.4)
OPIRL	<b>-13.8(±1.7)</b>	<b>1875.6(±1837.4)</b>	<b>622.5(±5.1)</b>
Ground-truth	-8.4(±2.2)	5419.4(±64.8)	729.9(±9.1)

IRL algorithms could achieve a policy with near-optimal performance when the environment structure changed. This was caused by multiple factors such as insufficient number of interactions and not reconstructing optimal reward functions during training on the source environment.

We also visualize the learned reward of OPIRL in Fig. 4. We can see that the learned reward function generalizes well to the unseen environment (see Fig. 3) and different goal positions.

For the second task, we tested different algorithms on a quadrupedal ant agent, which is a modified version of OpenAI’s Gym Ant-v2. During reward training, the agent is trained on a regular quadruped-ant environment (see Fig. 3c), then we modify the agent in two ways. The BigAnt (see Fig. 3d) is an environment introduced in Transfer Learning Environment<sup>3</sup>, where the length of all legs are doubled. The Amputated Ant (see Fig. 3e), on the other hand, has two shortened and disabled front legs that can significantly change the gait. As seen in Table I, OPIRL successfully recovers a near-optimal performance compared to other IRL methods. IL methods, which require direct policy generalization, fail to move forward in either task, even though they achieve near-optimal performance on the source environment. This is due to over-fitting to the trained environment and not learning the underlying goal of the new task.

## VI. ABLATION EXPERIMENTS

In this section, we perform a series of ablation experiments to understand what components contribute to the perfor-

mance gain.

### A. Reward Function

Instead of using the specific discriminator and the reward function formulation proposed in Sec. IV-B, we evaluate the performance of them with different formulations. Specifically, we run experiments on policy performance tasks with the following implicit/explicit reward functions:

$$r(s, a) = -\log(1 - D_{\theta, \omega, \Phi}(s, a)), \quad (17)$$

which *implicitly* infers the reward function as proposed in GAIL [5], and

$$\begin{aligned} r(s, a) &= \log D_{\theta, \omega, \Phi}(s, a) - \log(1 - D_{\theta, \omega, \Phi}(s, a)) \\ &= h_{\omega, \Phi}(s, a) - \log \pi_{\theta}(a|s), \end{aligned} \quad (18)$$

designed to explicitly learn the reward function in AIRL [7], where the discriminator takes the same form as Eq. (3). The shape of the implicit reward function in Eq. (17) is also used in OPOLO. Hence, Eq. (17) is a variant of OPOLO. Note that, OPOLO learns via only the state distribution, whereas here we train the agent using state-action distribution. It is noted that Eq. (18) differs from our formulation since our proposed method does not includes an entropy regularization (see Eq. (13)).

We show the results in Fig. 5. OPIRL combined with the implicit reward function of GAIL shows competitive results from our original OPIRL. However, as we cannot recover the reward function in this implicit formulation, we can conclude that OPIRL can be a more superior choice. On the other hand, OPIRL combined with explicit reward function of AIRL fails to learn in all scenarios.

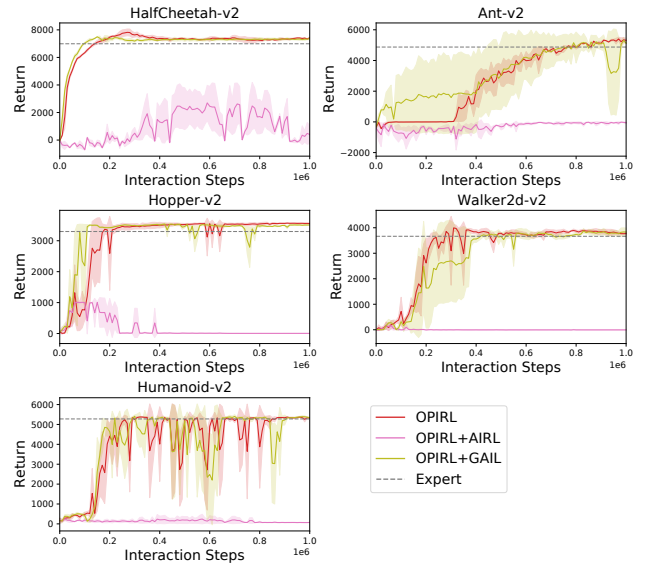


Fig. 5: Learning curves of OPIRL with different types of reward functions. Our formulation (Eq.(13)) achieves the best score, along with OPIRL+GAIL.

<sup>3</sup><https://github.com/seba-1511/shapechanger>



TABLE II: Comparison between the average return of the trained policy vs that of the expert policy using  $\{1, 4, 16\}$  trajectories for 1M environment steps. The table reports the mean and standard deviation of returns for 3 random seeds which were evaluated using 20 episodes. The bold number indicates the best score among each algorithm.

# Exp Traj	Method	HalfCheetah	Ant	Walker-2D	Hopper	Humanoid
1	BC	-254.4( $\pm 214.3$ )	-731.4( $\pm 192.8$ )	256.3( $\pm 23.6$ )	2957.7( $\pm 332.2$ )	448.9( $\pm 22.1$ )
	DAC	7398.1( $\pm 45.4$ )	5704.0( $\pm 107.3$ )	3789.2( $\pm 36.9$ )	3483.9( $\pm 16.1$ )	5134.4( $\pm 325.4$ )
	OPOLO	7299.1( $\pm 29.3$ )	<b>5799.4(<math>\pm 178.0</math>)</b>	3761.1( $\pm 94.2$ )	3373.9( $\pm 184.8$ )	194.0( $\pm 7.6$ )
	AIRL	1811.4( $\pm 1138.3$ )	-73.1( $\pm 73.5$ )	526.7( $\pm 66.6$ )	23.8( $\pm 12.9$ )	168.3( $\pm 107.4$ )
	<i>f</i> -IRL	<b>8200.5(<math>\pm 113.8</math>)</b>	3080.0( $\pm 36.5$ )	1104.9( $\pm 889.2$ )	2176.8( $\pm 1414.6$ )	4542.3( $\pm 1042.5$ )
	OPIRL (w/o Reg)	7337.2( $\pm 114.2$ )	2560.9( $\pm 1915.4$ )	<b>3824.1(<math>\pm 89.1</math>)</b>	<b>3554.87(<math>\pm 55.29</math>)</b>	<b>5318.7(<math>\pm 20.8</math>)</b>
	OPIRL	7416.1( $\pm 59.2$ )	5315.2( $\pm 141.4$ )	3771.1( $\pm 42.5$ )	<b>3558.3(<math>\pm 14.9</math>)</b>	<b>5335.8(<math>\pm 23.0</math>)</b>
4	BC	3629.1( $\pm 1513.4$ )	-596.6( $\pm 341.7$ )	2175.0( $\pm 530.0$ )	2347.8( $\pm 1334.9$ )	524.8( $\pm 98.2$ )
	DAC	7302.3( $\pm 80.2$ )	5361.5( $\pm 211.9$ )	<b>3921.5(<math>\pm 92.1</math>)</b>	2361.7( $\pm 1661.0$ )	<b>5358.6(<math>\pm 18.1</math>)</b>
	OPOLO	7321.6( $\pm 116.3$ )	<b>5568.9(<math>\pm 298.1</math>)</b>	3863.3( $\pm 40.6$ )	3211.8( $\pm 245.7$ )	227.8( $\pm 101.1$ )
	AIRL	1376.8( $\pm 1233.0$ )	57.4( $\pm 28.9$ )	552.2( $\pm 104.2$ )	7.2( $\pm 2.3$ )	122.1( $\pm 17.4$ )
	<i>f</i> -IRL	<b>7501.9(<math>\pm 470.6</math>)</b>	3217.0( $\pm 232.6$ )	2181.1( $\pm 437.3$ )	3208.3( $\pm 112.3$ )	4098.1( $\pm 1775.8$ )
	OPIRL	7114.9( $\pm 211.4$ )	3916.3( $\pm 1105.9$ )	3549.3( $\pm 30.7$ )	<b>3827.7(<math>\pm 110.3</math>)</b>	5259.0( $\pm 118.5$ )
	BC	7228.5( $\pm 152.3$ )	4358.5( $\pm 524.2$ )	3779.7( $\pm 23.5$ )	3552.4( $\pm 9.5$ )	4696.8( $\pm 243.7$ )
16	DAC	7254.3( $\pm 149.5$ )	5351.5( $\pm 250.0$ )	3539.4( $\pm 1.4$ )	<b>3827.4(<math>\pm 86.1</math>)</b>	<b>5338.1(<math>\pm 43.7</math>)</b>
	OPOLO	<b>7401.2(<math>\pm 68.3</math>)</b>	<b>5758.3(<math>\pm 406.0</math>)</b>	<b>3827.4(<math>\pm 86.1</math>)</b>	3539.4( $\pm 1.4$ )	403.1( $\pm 88.1$ )
	AIRL	1244.9( $\pm 1407.6$ )	23.1( $\pm 2.3$ )	624.4( $\pm 167.6$ )	48.8( $\pm 42.7$ )	158.3( $\pm 77.4$ )
	<i>f</i> -IRL	7108.9( $\pm 192.8$ )	3126.4( $\pm 700.5$ )	1534.9( $\pm 929.3$ )	3228.4( $\pm 217.3$ )	<b>5379.0(<math>\pm 96.9</math>)</b>
	OPIRL	7187.0( $\pm 3.5$ )	4909.3( $\pm 545.0$ )	3777.7( $\pm 58.7$ )	3701.2( $\pm 139.5$ )	<b>5353.9(<math>\pm 14.3</math>)</b>
Expert	SAC	6991.7( $\pm 124.3$ )	4875.1( $\pm 1036.8$ )	3665.1( $\pm 527.2$ )	3298.7( $\pm 433.2$ )	5277.2( $\pm 490.7$ )

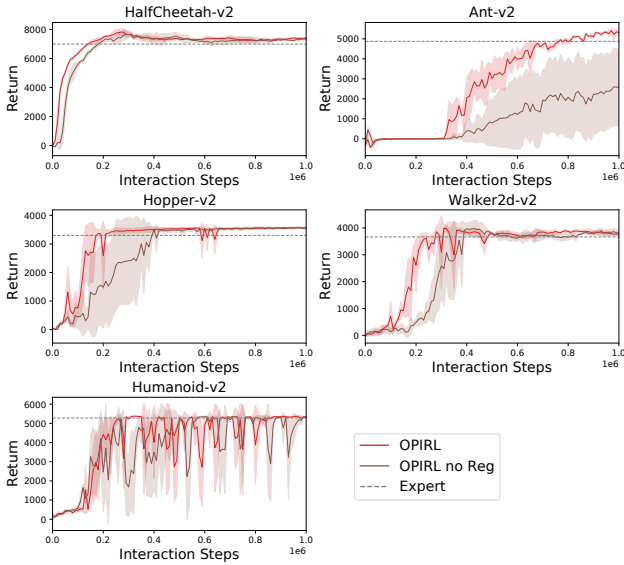


Fig. 6: Learning curves of OPIRL with and without BC loss+Q-Filter. Applying BC Loss+Q-Filter enables the agent to explore more widely at the beginning stages of training, thus converging faster than the agent without such regularization.

### B. Effects of Behavior Cloning Loss and Q-Filter

We then investigate how the regularization works. As reverse KL-Divergence is known to be mode-seeking, we adopt behavior cloning loss to encourage mode-covering behaviors as described in Sec. IV-C. Fig. 6 plots the results, and we can see that BC loss enables our algorithm to reach expert-level performance in fewer environment steps. This impact is especially prominent in Ant-V2 environment, where our algorithm without the BC loss cannot converge in the given training steps.

### C. Number of Trajectories

We run experiments on multiple trajectories to provide evidence that our algorithm shows robust results even on a single expert demonstration. All three off-policy based methods, DAC, OPOLO, and OPIRL, show consecutive high performance on all experiments. BC also shows decent performance when provided with ample expert trajectories, a behavior seen in prior work [24]. AIRL, however, cannot achieve high performance even with 16 expert trajectories due to lack of environment interactions (1M steps). *f*-IRL, although showing decent performance on all tasks, could not reach expert-level on complicated tasks such as Ant and Walker. In all scenarios, we can observe that OPIRL is far more sample-efficient than AIRL.

## VII. CONCLUSION

Imitation learning and inverse reinforcement learning have eliminated hand-crafted reward design, which requires tremendous effort or is even infeasible in complex systems. However, we have seen that prior works of the former cannot generalize to different environments, and the latter requires a massive number of interactions with environments. In this paper, we propose OPIRL that has the two desired properties: high sample efficiency and generalization capability to unseen environments. To achieve this, OPIRL combines three main components: 1) adopts off-policy data distribution, 2) leverages mode-covering behavior for faster training, and 3) learns a stationary reward function. Our experiments demonstrated that OPIRL can achieve comparable or better sample efficiency among state-of-the-art IL and IRL methods with the limited data regime. In addition, it achieves the highest performance on novel environments.

In the future, we plan to expand the usability of our algorithm to more complicated settings, such as high dimensional

inputs (e.g., images, videos). We also aim to investigate how we can make use of the proposed method for controlling real systems.

## VIII. ACKNOWLEDGMENT

This work is supported by JST CREST Grant Number JPMJCR19F5.

## REFERENCES

- [1] D. Amodei, C. Olah, J. Steinhardt, P. Christiano, J. Schulman, and D. Mané, "Concrete Problems in AI Safety," *arXiv:1606.06565 [cs]*, 2016.
- [2] D. Hadfield-Menell, S. J. Russell, P. Abbeel, and A. Dragan, "Cooperative Inverse Reinforcement Learning," in *Advances in Neural Information Processing Systems*, vol. 29, 2016.
- [3] M. Teranishi, K. Fujii, and K. Takeda, "Trajectory prediction with imitation learning reflecting defensive evaluation in team sports," in *2020 IEEE 9th Global Conference on Consumer Electronics (GCCE)*, 2020.
- [4] M. Bojarski, D. Del Testa, D. Dworakowski, B. Firner, B. Flepp, P. Goyal, L. D. Jackel, M. Monfort, U. Muller, J. Zhang, X. Zhang, J. Zhao, and K. Zieba, "End to End Learning for Self-Driving Cars," *arXiv:1604.07316 [cs]*, 2016.
- [5] J. Ho and S. Ermon, "Generative Adversarial Imitation Learning," in *Advances in Neural Information Processing Systems*, vol. 29, 2016.
- [6] I. Goodfellow, J. Pouget-Abadie, M. Mirza, B. Xu, D. Warde-Farley, S. Ozair, A. Courville, and Y. Bengio, "Generative Adversarial Nets," in *Advances in Neural Information Processing Systems*, vol. 27, 2014.
- [7] J. Fu, K. Luo, and S. Levine, "Learning Robust Rewards with Adversarial Inverse Reinforcement Learning," in *International Conference on Learning Representations*, 2018.
- [8] L. Yu, T. Yu, C. Finn, and S. Ermon, "Meta-Inverse Reinforcement Learning with Probabilistic Context Variables," in *Advances in Neural Information Processing Systems*, vol. 32, 2019.
- [9] S. Russell, "Learning agents for uncertain environments," in *Proceedings of the eleventh annual conference on Computational learning theory - COLT'98*, 1998.
- [10] A. Y. Ng and S. Russell, "Algorithms for Inverse Reinforcement Learning," in *17th International Conference on Machine Learning*, 2000.
- [11] P. Abbeel and A. Y. Ng, "Apprenticeship learning via inverse reinforcement learning," in *21st international Conference on Machine Learning - ICML '04*, 2004.
- [12] I. Kostrikov, K. K. Agrawal, D. Dwibedi, S. Levine, and J. Tompson, "Discriminator-Actor-Critic: Addressing Sample Inefficiency and Reward Bias in Adversarial Imitation Learning," in *International Conference on Learning Representations*, 2018.
- [13] Z. Wu, L. Sun, W. Zhan, C. Yang, and M. Tomizuka, "Efficient Sampling-Based Maximum Entropy Inverse Reinforcement Learning with Application to Autonomous Driving," *IEEE Robotics and Automation Letters*, vol. 5, 2020.
- [14] J. Schulman, F. Wolski, P. Dhariwal, A. Radford, and O. Klimov, "Proximal Policy Optimization Algorithms," *arXiv:1707.06347 [cs]*, 2017.
- [15] L. Blondé and A. Kalousis, "Sample-Efficient Imitation Learning via Generative Adversarial Nets," in *The 22nd International Conference on Artificial Intelligence and Statistics*, 2019.
- [16] F. Sasaki, T. Yohira, and A. Kawaguchi, "Sample Efficient Imitation Learning for Continuous Control," in *International Conference on Learning Representations*, 2018.
- [17] I. Kostrikov, O. Nachum, and J. Tompson, "Imitation Learning via Off-Policy Distribution Matching," in *International Conference on Learning Representations*, 2019.
- [18] Z. Zhu, K. Lin, B. Dai, and J. Zhou, "Off-Policy Imitation Learning from Observations," in *Advances in Neural Information Processing Systems*, vol. 33, 2021.
- [19] S. K. S. Ghasemipour, R. Zemel, and S. Gu, "A Divergence Minimization Perspective on Imitation Learning Methods," in *Conference on Robot Learning*, 2019.
- [20] O. Nachum, M. Norouzi, and D. Schuurmans, "Improving Policy Gradient by Exploring Under-appreciated Rewards," 2016.
- [21] A. Nair, B. McGrew, M. Andrychowicz, W. Zaremba, and P. Abbeel, "Overcoming Exploration in Reinforcement Learning with Demonstrations," *IEEE International Conference on Robotics and Automation*, 2018.
- [22] B. D. Ziebart, A. Maas, J. A. Bagnell, and A. K. Dey, "Maximum Entropy Inverse Reinforcement Learning," *Proceedings of the 23rd national conference on Artificial intelligence*.
- [23] C. Finn, S. Levine, and P. Abbeel, "Guided Cost Learning: Deep Inverse Optimal Control via Policy Optimization," in *Proceedings of the 33rd International Conference on International Conference on Machine Learning - Volume 48*, 2016.
- [24] T. Ni, H. Sikchi, Y. Wang, T. Gupta, L. Lee, and B. Eysenbach, "f-IRL: Inverse Reinforcement Learning via State Marginal Matching," *Conference on Robot Learning*, 2020.
- [25] O. Nachum, Y. Chow, B. Dai, and L. Li, "DualDICE: Efficient Estimation of Off-Policy Stationary Distribution Corrections," *ICML 2019 Workshop RL4RealLife Paper32*, 2019.
- [26] M. Sun, A. Mahajan, K. Hofmann, and S. Whiteson, "SoftDICE for Imitation Learning: Rethinking Off-policy Distribution Matching," *arXiv:2106.03155 [cs]*, 2021.
- [27] L.-J. Lin, "Self-improving reactive agents based on reinforcement learning, planning and teaching," *Machine Learning*, vol. 8, no. 3, 1992.
- [28] O. Nachum, B. Dai, I. Kostrikov, Y. Chow, L. Li, and D. Schuurmans, "AlgaeDICE: Policy Gradient from Arbitrary Experience," *Optimization Foundations for Reinforcement Learning Workshop at NeurIPS 2019*, 2019.
- [29] L. Yu, J. Song, and S. Ermon, "Multi-Agent Adversarial Inverse Reinforcement Learning," in *International Conference on Machine Learning*, 2019.
- [30] S. Y. Arnob, "Off-Policy Adversarial Inverse Reinforcement Learning," *arXiv:2005.01138 [cs, stat]*, 2020.
- [31] T. Haarnoja, H. Tang, P. Abbeel, and S. Levine, "Reinforcement Learning with Deep Energy-Based Policies," *arXiv:1702.08165 [cs]*, 2017.
- [32] T. Haarnoja, A. Zhou, P. Abbeel, and S. Levine, "Soft Actor-Critic: Off-Policy Maximum Entropy Deep Reinforcement Learning with a Stochastic Actor," *arXiv:1801.01290 [cs, stat]*, 2018.
- [33] B. Wu, F. Xu, Z. He, A. Gupta, and P. K. Allen, "SQUIRL: Robust and Efficient Learning from Video Demonstration of Long-Horizon Robotic Manipulation Tasks," *IEEE/RSJ International Conference on Intelligent Robots and Systems*, 2020.
- [34] K. Ota, D. K. Jha, T. Oiki, M. Miura, T. Nammoto, D. Nikovski, and T. Mariyama, "Trajectory Optimization for Unknown Constrained Systems using Reinforcement Learning," *International Conference on Intelligent Robots and System*, 2020.
- [35] E. Todorov, T. Erez, and Y. Tassa, "MuJoCo: A physics engine for model-based control," in *2012 IEEE/RSJ International Conference on Intelligent Robots and Systems*, 2012.
- [36] T. Miyato, T. Kataoka, M. Koyama, and Y. Yoshida, "Spectral Normalization for Generative Adversarial Networks," in *arXiv:1802.05957 [cs, stat]*, 2018.
- [37] H. Zhang, M. Cisse, Y. N. Dauphin, and D. Lopez-Paz, "mixup: Beyond Empirical Risk Minimization," in *arXiv:1710.09412 [cs, stat]*, 2018.
- [38] A. S. Chen, H. Nam, S. Nair, and C. Finn, "Batch Exploration with Examples for Scalable Robotic Reinforcement Learning," *IEEE Robotics and Automation Letters*, vol. 6, no. 3, 2021.
- [39] K. Xu, E. Ratner, A. Dragan, S. Levine, and C. Finn, "Learning a Prior over Intent via Meta-Inverse Reinforcement Learning," in *International Conference on Machine Learning*, 2019.
- [40] M. Orsini, A. Raichuk, L. Hussenot, D. Vincent, R. Dadashi, S. Girgin, M. Geist, O. Bachem, O. Pietquin, and M. Andrychowicz, "What Matters for Adversarial Imitation Learning?" *arXiv:2106.00672 [cs]*, 2021.
- [41] L. Blondé, P. Strasser, and A. Kalousis, "Lipschitzness Is All You Need To Tame Off-policy Generative Adversarial Imitation Learning," *arXiv:2006.16785 [cs]*, 2021.
- [42] V. Nair and G. E. Hinton, "Rectified linear units improve restricted boltzmann machines," in *Proceedings of the 27th International Conference on International Conference on Machine Learning*, ser. ICML '10, 2010.
- [43] D. P. Kingma and J. Ba, "Adam: A Method for Stochastic Optimization," *arXiv:1412.6980 [cs]*, 2017.



- [44] I. Gulrajani, F. Ahmed, M. Arjovsky, V. Dumoulin, and A. Courville, “Improved Training of Wasserstein GANs,” in *Advances in Neural Information Processing Systems*, vol. 30, 2017.
- [45] K. Ota, “TF2RL,” 2020.
- [46] G. Brockman, V. Cheung, L. Pettersson, J. Schneider, J. Schulman, J. Tang, and W. Zaremba, “OpenAI Gym,” *arXiv:1606.01540 [cs]*, 2016.
- [47] A. H. Qureshi, B. Boots, and M. C. Yip, “Adversarial Imitation via Variational Inverse Reinforcement Learning,” *arXiv:1809.06404 [cs, stat]*, 2019.

## APPENDIX I PROOF

### A. Derivation of KL-Divergence Upper-bound

Inspired by the works of [18, 28] we set an upper-bound on KL-divergence using  $f$ -divergence. For two arbitrary distributions  $P$  and  $Q$ , using the Jensen’s inequality, the upper bound of KL-divergence can be shown as  $D_{KL}[P\|Q] \leq D_f[P\|Q]$ :

$$\begin{aligned} D_{KL}[P\|Q] &= \int p(x) \log \frac{p(x)}{q(x)} dx \\ &\leq \log \int \frac{p^2(x)}{q(x)} dx \\ &\leq \frac{1}{2} \int \frac{p^2(x)}{q(x)} dx = D_f[P\|Q] \end{aligned} \quad (19)$$

where  $f(x) = \frac{1}{p}|x|^p$ . From prior empirical results [28], in our work we use  $f(x) = \frac{1}{2}x^{3/2}$  for a tighter upper bound.

### B. Derivation of our Eq.(12)

We show the equation transformation from on-policy training to off-policy training in Eq. (12) in the main paper. Recall that the Bellman equation for state-action Q-function is  $\mathcal{B}^\pi Q(s, a) = \mathbb{E}_{s' \sim P(s, a), a' \sim \pi(s')} [r(s, a) + \gamma Q(s', a')]$ , and  $r(s, a) = \log \frac{\rho^{\text{exp}}(s, a)}{\rho^R(s, a)}$ . The RHS of the equation

$$\begin{aligned} J(\pi, Q) &= \mathbb{E}_{\rho^{\pi_\theta}} \left[ \log \frac{\rho^{\text{exp}}(s, a)}{\rho^R(s, a)} - (\mathcal{B}^\pi Q - Q)(s, a) \right] \\ &\quad + \mathbb{E}_{\rho^R} [f_*((\mathcal{B}^\pi Q - Q)(s, a))] \end{aligned} \quad (20)$$

can be expressed via initial state and actions in the following manner:

$$\begin{aligned} &\mathbb{E}_{\rho^{\pi_\theta}} \left[ \log \frac{\rho^{\text{exp}}(s, a)}{\rho^R(s, a)} - (\mathcal{B}^\pi Q - Q)(s, a) \right] \\ \Leftrightarrow &\mathbb{E}_{\rho^{\pi_\theta}} [r(s, a) - Q(s, a) - \mathbb{E}_{s' \sim P(s, a)} [\mathcal{B}^\pi Q(s, a)]] \\ \Leftrightarrow &\mathbb{E}_{\rho^{\pi_\theta}} [r(s, a) + Q(s, a) \\ &\quad - \mathbb{E}_{s' \sim P(s, a), a' \sim \pi(s)} [r(s, a) + \gamma Q(s', a')]] \\ \Leftrightarrow &\mathbb{E}_{\rho^{\pi_\theta}} [Q(s, a) - \gamma \mathbb{E}_{s' \sim P(s, a), a' \sim \pi(s)} [Q(s', a')]] \\ \Leftrightarrow &(1 - \gamma) \sum_{t=0}^{\infty} \gamma^t \mathbb{E}_{s \sim \rho_t^{\pi_\theta}, a \sim \pi(s)} [Q(s, a)] \\ &\quad - (1 - \gamma) \sum_{t=0}^{\infty} \gamma^{t+1} \mathbb{E}_{s' \sim P(s, a), a' \sim \pi(s')} [Q(s', a')] \\ \Leftrightarrow &(1 - \gamma) \sum_{t=0}^{\infty} \gamma^t \mathbb{E}_{s \sim \rho_t^{\pi_\theta}, a \sim \pi(s)} [Q(s, a)] \\ &\quad - (1 - \gamma) \sum_{t=0}^{\infty} \gamma^{t+1} \mathbb{E}_{s' \sim \rho_{t+1}^{\pi_\theta}, a' \sim \pi(s')} [Q(s', a')] \\ \Leftrightarrow &(1 - \gamma) \mathbb{E}_{s_0 \sim \rho_0^{\pi_\theta}, a_0 \sim \pi(s_0)} [Q(s_0, a_0)]. \end{aligned} \quad (21)$$

Therefore, combining it with LHS, we get the objective function defined in Eq. (12):

$$\begin{aligned} \max_{\pi} \min_{x: S \times \mathcal{A} \rightarrow R} J(\pi, x) \\ &= \max_{\pi} \min_{Q: S \times \mathcal{A} \rightarrow R} J(\pi, Q) \\ &= (1 - \gamma) \mathbb{E}_{s_0, a_0} [Q(s_0, a_0)] + \mathbb{E}_{\rho^R} [f_*((\mathcal{B}^\pi Q - Q)(s, a))]. \end{aligned} \quad (22)$$

## APPENDIX II EXPERIMENT DETAILS

In this section, we provide details on our experiments.

### A. Implementation Details

All networks are structured using a 2-layer fully-connected network. For reward functions we use 64 hidden units with ReLU activation [42], and 256 for other networks. All networks uses Adam optimizer [43] with  $10^{-5}$  for actor and discriminator network, and  $10^{-3}$  for critic network for all tasks except for HalfCheetah-v2 where the discriminator uses  $3 \times 10^{-4}$ . The actor loss regularization coefficient and behavior cloning loss regularization coefficient uses  $10^{-3}$  and  $1/\text{batch\_size}$  respectively, where the batch size is set to 256 for all tasks. We use absorbing states of the environments following the works of Kostrikov et al. [12] and normalize states for stable training. Therefore, the replay buffer size is set to  $2 \times \text{total\_timesteps}$  where the total timesteps is set to  $10^6$  for all policy performance tasks. For transfer learning, we train the reward functions for  $5 \times 10^5$  to avoid over-fitting to the current policy. Furthermore, we used 16 trajectories for PointMaze task to increase the variety of goal position.

We use gradient penalty [44] to enhance stable training for discriminators in reward training. In our policy update, following the technique used in AlgaeDICE [28], we mix the Q-value function  $Q_\phi(s', a')$  in Eq. (16) with target Q-value

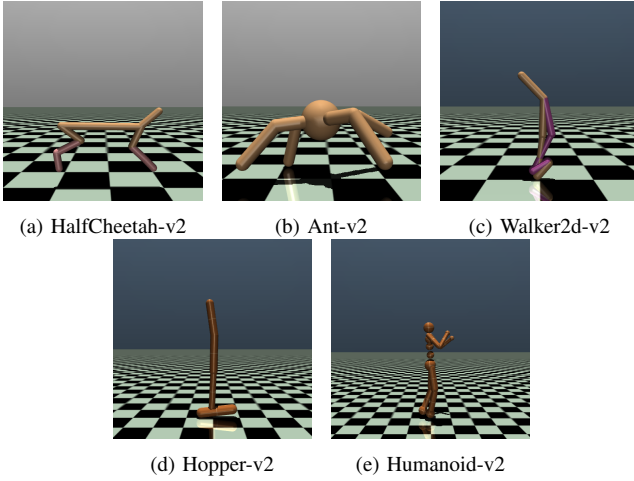


Fig. 7: Environments used in policy performance evaluation tasks.

$\bar{Q}_\phi(s', a')$  as follows:

$$\lambda_3 Q_\phi(s', a') + (1 - \lambda_3) \bar{Q}_\phi(s', a'). \quad (23)$$

where  $\lambda_3$  is set to 0.05. All expert demonstrations were collected via training an agent using Soft-Actor-Critic [32] using the library TF2RL<sup>4</sup> [45].

We emphasize that our method requires minimal hyperparameter tuning. In contrast, prior arts such as AIRL, require excessive tuning, and minor difference can cause the training to fail.

For OPOLO [18] and  $f$ -IRL [24], we use its original implementations and hyperparameters.

### B. Environments

For policy performance tasks, we use 5 continual control tasks from OpenAI Gym [46] simulated on a physics simulator MuJoCo [35]: HalfCheetah-v2, Ant-v2, Walker2d-v2, Hopper-v2, and Humanoid-v2 (See Fig. 7).

Environments for transfer learning tasks involves the point-mass environment, and quadrupedal ant environment introduced in the original AIRL paper [7]. In addition, we use an extension of the quadrupedal ant environment, where the length of all legs are double, which was also done in prior works [47].

### C. Transfer Learning Visualization Results

We visualize the movement of the agents on both source and target environment in Fig. 8 and Fig. 9. In PointMaze environments, we can observe that both agents successfully learn to reach the goal in spite of differences in position of the border. Similarly, in quadrupedal Ant environment, BigAnt successfully learns to move from left to right in the same manner as the source environment. However, due to two front legs being shortened, it is difficult for AmputatedAnt to move like the other models. Thus, it has to rotate to achieve smooth sideways movement.

### D. Additional Experiment Results

We show additional information on sample efficiency comparison between IRL methods: OPIRL vs  $f$ -IRL. We extract the learning curves of the two methods from Fig. 2 and plot the lines until it reaches the expert level for a couple of steps. As shown in Fig. 10 we can observe that our method significantly improves the sample efficiency for all tasks. This is especially prominent on more complicated tasks such as Humanoid.

Furthermore, We show the learning curves for multiple trajectory results in Fig. 11 and Fig. 12. In all experiments, OPIRL DAC, and OPOLO show comparable results, except for OPIRL on Ant environment.  $f$ -IRL shows decent performance on all tasks, however it cannot reach optimal level within 1M steps threshold. BC performance increases as the number of trajectory grows. This result is expected, and also seen in prior work [24]. For AIRL, although tuning the learning rates, it failed on almost all tasks, except for HalfCheetah and Walker2D.

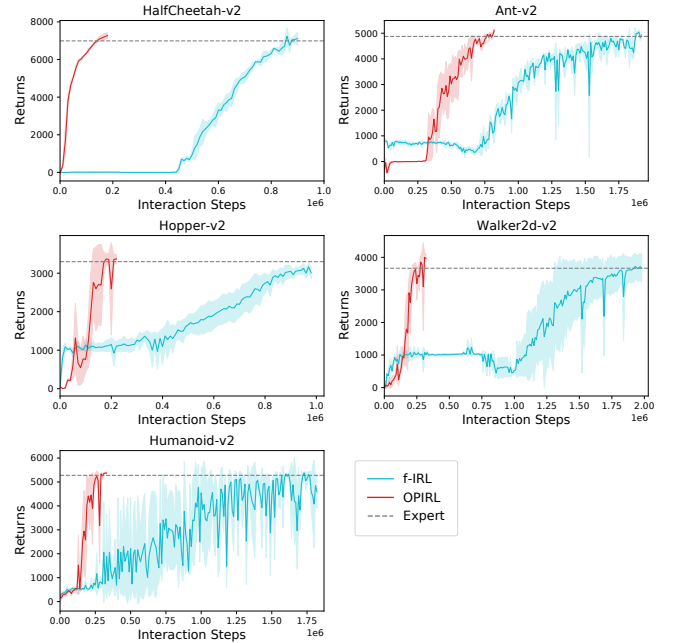


Fig. 10: Comparison between our method and  $f$ -IRL. We show the training curve until it reaches the expert level for couple of steps. OPIRL reaches expert-level performance in significantly less steps than  $f$ -IRL.

<sup>4</sup><https://github.com/keiohta/tf2rl/>

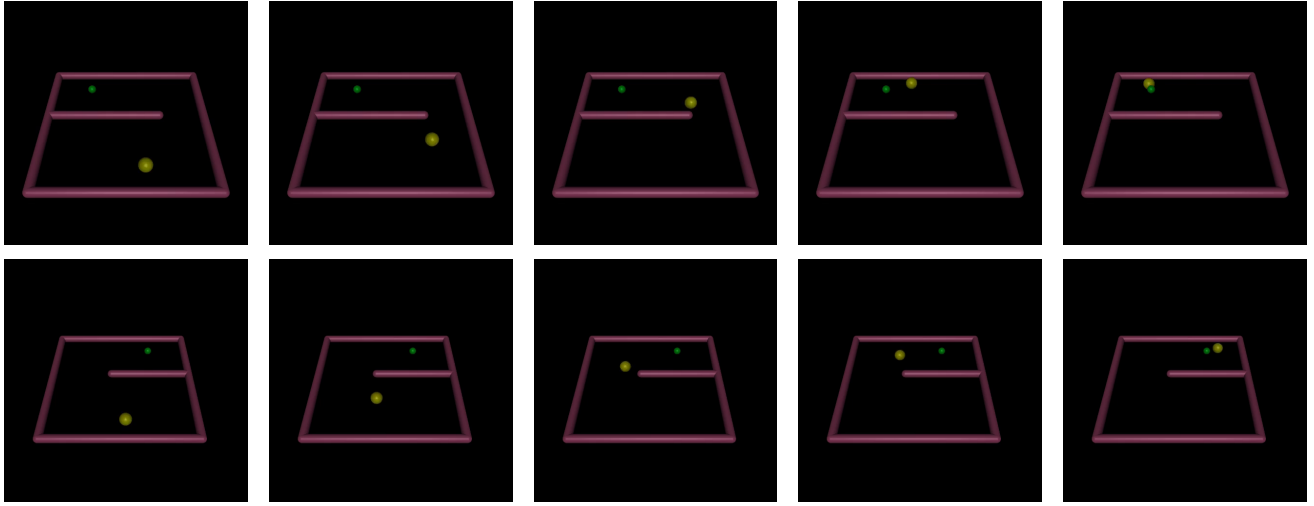


Fig. 8: **Top row:** The original PointMaze-Left, where the ball (yellow) tries to reach the goal (green). **Bottom row:** OPIRL successfully learns a new policy on PointMaze-Right via transferring the reward learned on the source environment.

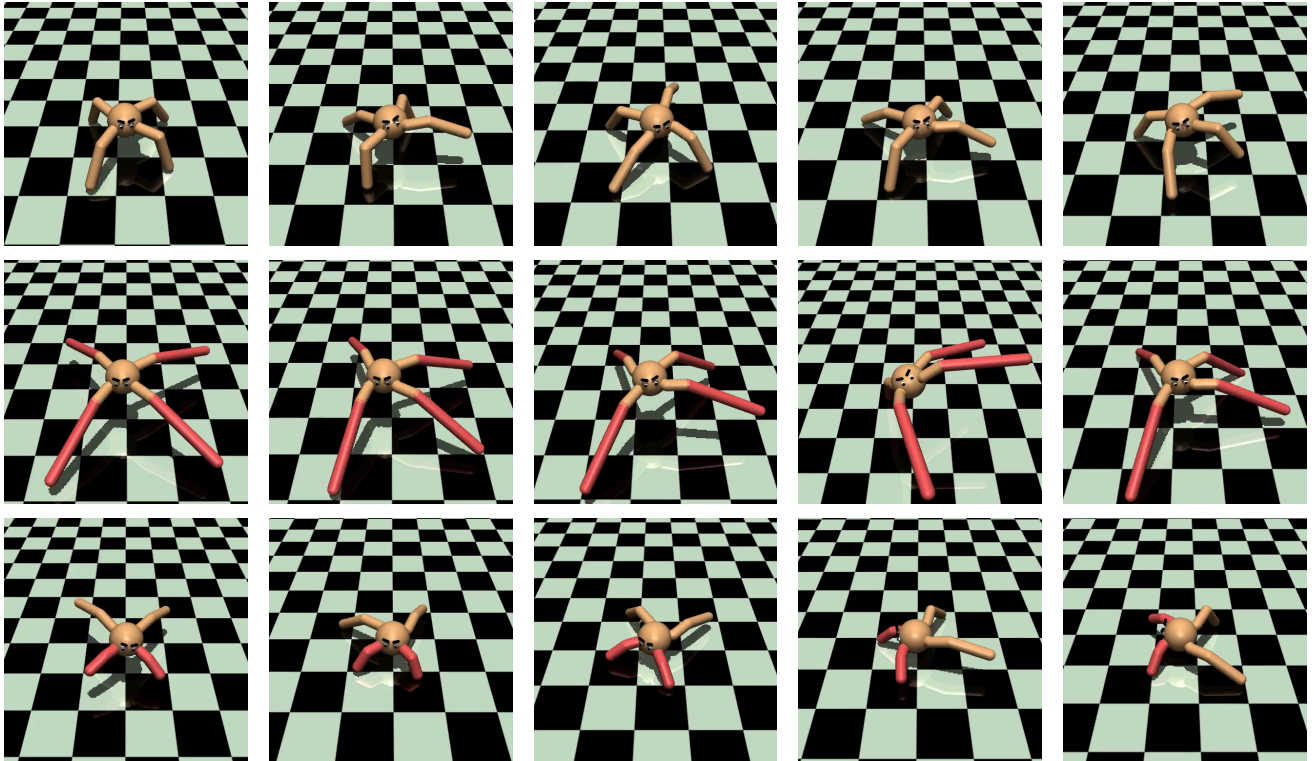


Fig. 9: **Top row:** The original quadrupedal ant moving from left to right. **Middle row:** BigAnt with successfully learning the policy with transferred reward function from the original quadrupedal ant. **Bottom row:** AmputatedAnt moving from left to right. Due to the amputated legs, it cannot move like the other environments, instead it turns backward to move in the right direction.

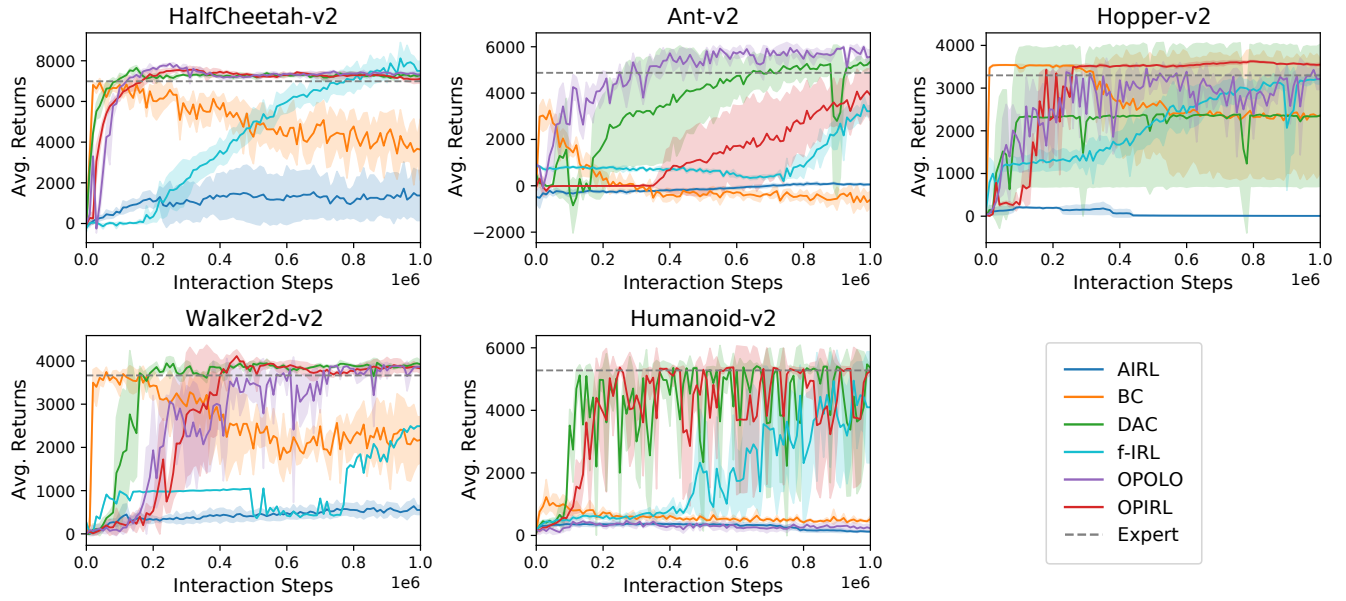


Fig. 11: Comparison between the average return of the trained policy vs that of the expert policy using 4 trajectory. The expert policy performance is shown in a gray horizontal line, and we run each agent on 3 seeds and plot the mean and standard deviation.

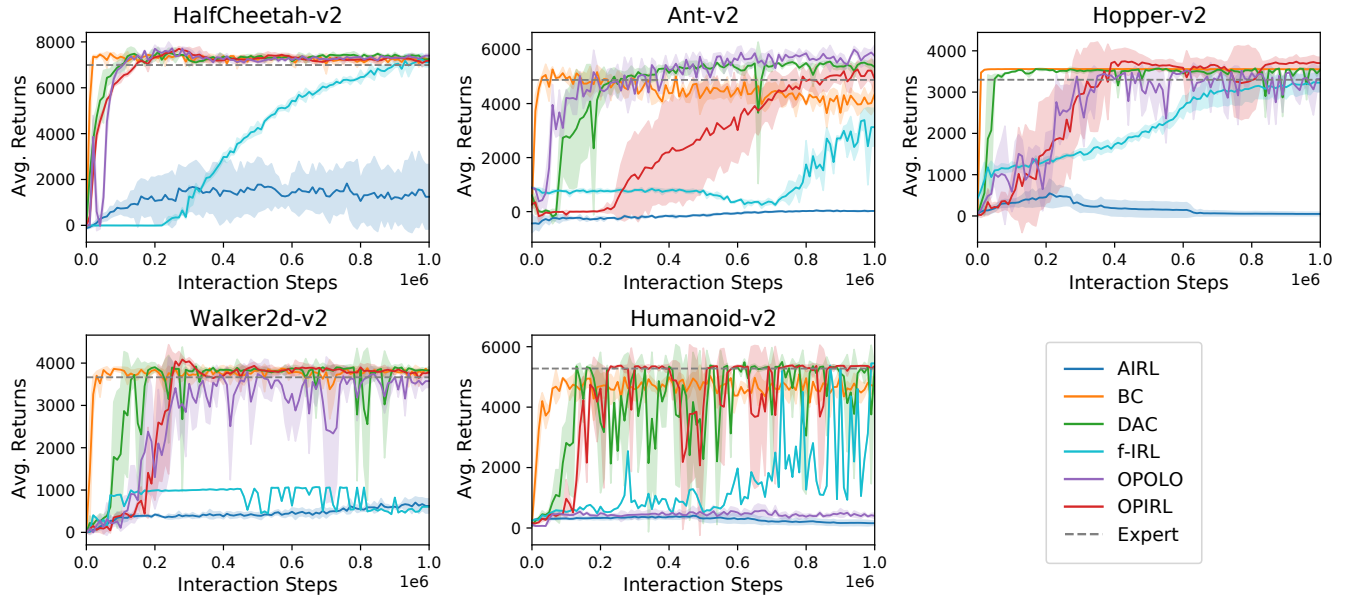


Fig. 12: Comparison between the average return of the trained policy vs that of the expert policy using 16 trajectory. The expert policy performance is shown in a gray horizontal line, and we run each agent on 3 seeds and plot the mean and standard deviation.